NR2 subunit-dependence of NMDA receptor channel block by external Mg^{2+}

Anqi Qian, Amy L. Buller and Jon W. Johnson

Department of Neuroscience, University of Pittsburgh, Pittsburgh, PA 15260, USA

The vital roles played by NMDA receptors in CNS physiology depend critically on powerful voltage-dependent channel block by external Mg^{2+} (Mg_o^{2+}). NMDA receptor channel block by Mg_o^{2+} depends on receptor subunit composition: NR1/2A receptors (receptors composed of NR1 and NR2A subunits) and NR1/2B receptors are more strongly inhibited by Mg_o^{2+} than are NR1/2C or NR1/2D receptors. We investigated the effects of Mg_o^{2+} on single-channel and whole-cell currents recorded from recombinant NR1/2D and NR1/2A receptors expressed in HEK293 and 293T cells. The main conclusions are as follows. (1) Voltage-dependent inhibition by Mg_o^{2+} of whole-cell NR1/2D receptor responses was at least 4-fold weaker than inhibition of NR1/2A receptor responses at all voltages tested. (2) Channel block by Mg_o^{2+} reduced the duration of NR1/2D receptor single-channel openings; this reduction was used to estimate the apparent blocking rate of Mg_o^{2+} ($k_{+,app}$). The $k_{+,app}$ for NR1/2D receptors was similar to but moderately slower than the $k_{+,app}$ obtained from cortical NMDA receptors composed of NR1, NR2A and NR2B subunits at all voltages tested. (3) Mg_o^{2+} blocking events induced an additional component in the closed-duration distribution; this component was used to estimate the apparent unblocking rate of Mg_o^{2+} ($k_{-,app}$). The $k_{-,app}$ for NR1/2D receptors was much faster than the $k_{-,app}$ for cortical receptors at all voltages tested. The voltage-dependence of the $k_{-,app}$ of NR1/2D and cortical receptors differed in a manner that suggested that Mg_o^{2+} may permeate NR1/2D receptors more easily than cortical receptors. (4) Mg_o^{2+} inhibits NR1/2D receptors less effectively than cortical receptors chiefly because Mg_o^{2+} unbinds much more rapidly from NR1/2D receptors.

(Resubmitted 4 October 2004; accepted after revision 27 October 2004; first published online 28 October 2004)
Corresponding author J. W. Johnson: Department of Neuroscience, 446 Crawford Hall, University of Pittsburgh, Pittsburgh, PA 15260, USA. Email: johnson@bns.pitt.edu

NMDA receptors comprise an ionotropic glutamate receptor subfamily that plays many critical roles in the vertebrate CNS. NMDA receptors are essential to the establishment and modification of synapses during development (Bear *et al.* 1990; Cline *et al.* 1990; Iwasato *et al.* 2000; Ramoa *et al.* 2001; Erisir & Harris, 2003), and to long-term modification of synaptic strength in adults, which underlies some types of learning and memory (Bliss & Collingridge, 1993; Tang *et al.* 1999; Lisman & McIntyre, 2001; Nakazawa *et al.* 2002). NMDA receptors are implicated in many diseases, including epilepsy, schizophrenia and neurodegerative disorders (Meldrum, 1992; Chapman, 2000; Cull-Candy *et al.* 2001; Tsai & Coyle, 2002; Zeron *et al.* 2002; Gardoni *et al.* 2003). Improved understanding of NMDA receptor function and regulation is of broad significance to nervous system physiology and pathology.

Functional NMDA receptors are believed generally to be heterotetramers of NR1 and NR2 subunits. There are four NR2 gene products, NR2A–NR2D. Expression of NR2 subunits follows distinct developmental and regional patterns of expression. For example, in rat cortex, NR2B subunits are present throughout development and in adult animals, while NR2A subunits are found postnatally. NR2D subunits appear prenatally, their expression peaks near postnatal day 7, and then expression decreases to adult levels (Monyer *et al.* 1994). NR2 subunit expression can be neurone-specific within brain structures; in the hippocampus, NR2A and 2B are the predominant subunits expressed in pyramidal cells while NR2C and 2D are the predominant subunits expressed in interneurones (Monyer *et al.* 1994). Different NR2 subunits even have distinct subcellular distributions, such as in cerebellar Golgi cells, where NR2A subunits are expressed both synaptically and extrasynaptically, while NR2D subunits are expressed predominantly at extrasynaptic sites (Brickley *et al.* 2003).

 DOI: 10.1113/jphysiol.2004.076737

This tight temporal and spatial control of NR2 subunit expression probably reflects the physiological importance of the NR2 subunit-dependence of NMDA receptor properties (Dingledine *et al.* 1999). Here, we focus on NMDA receptors composed of NR1 and NR2D subunits (NR1/2D receptors). Although not as extensively studied as NR1/2A and NR1/2B receptors, NR1/2D receptors are involved in many CNS processes, including stress pathways (Miyamoto *et al.* 2002), epileptogenesis (Bengzon *et al.* 1999) and synaptic plasticity (Okabe *et al.* 1998; Bengzon *et al.* 1999; Hrabetova *et al.* 2000). The basic pharmacological and biophysical properties of NR1/2D receptors have been characterized in expression systems and in carefully chosen native preparations. NR1/2D receptors have been shown to exhibit unique gating properties, including an extremely slow deactivation rate and an unequal probability in transitions between the main and subconductance states (Monyer *et al.* 1994; Wyllie *et al.* 1996, 1998; Vicini *et al.* 1998; Misra *et al.* 2000). In addition, the channel properties of NR1/2D (along with NR1/2C) receptors are distinct from the channel properties of NR1/2A or NR1/2B receptors. These properties include single-channel conductance, kinetics (Stern *et al.* 1992; Momiyama *et al.* 1996; Wyllie *et al.* 1996) and sensitivity to external Mg^{2+} (Mg_o^{2+}) block (Monyer *et al.* 1994; Kuner & Schoepfer, 1996).

Voltage-dependent channel block by Mg_o^{2+} (Mayer *et al.* 1984; Nowak *et al.* 1984; Ascher & Nowak, 1988) is an NMDA receptor property of fundamental physiological importance. In addition to its functional implications, block by Mg_o^{2+} provides a means to explore the structure and gating of NMDA receptors (see Johnson & Qian, 2002). The majority of work on Mg_o^{2+} block has been performed on NR1/2A or NR1/2B receptors using expression systems, or on native receptors which are most likely to contain NR1, NR2A and NR2B subunits. The studies that have addressed Mg_o^{2+} interaction with NR1/2D and NR1/2C receptors revealed that Mg_o^{2+} inhibits these receptors much less effectively than NR1/2A or NR1/2B receptors (e.g. Monyer *et al.* 1994; Kuner & Schoepfer, 1996). However, single-channel measurements of Mg_o^{2+} interaction with NR1/2D or NR1/2C receptors have not been reported. Such measurements are particularly challenging because of the brief open duration of NR1/2D and NR1/2C receptors (Stern *et al.* 1992; Wyllie *et al.* 1996, 1998), which is further shortened by Mg_o^{2+}. Consequently, basic properties of Mg_o^{2+} block of NR1/2D and NR1/2C receptors, including the magnitude and voltage-dependence of the rate of Mg_o^{2+} entry into and exit from their channels, were not known.

The goals of this study were 2-fold. The first goal was to perform an integrated whole-cell and single-channel study of Mg_o^{2+} block of NR1/2D receptors. While satisfying this goal we also characterized in a mammalian expression system the single-channel properties of NR1/NR2D receptors. The second goal was to explore the origin of the differences in Mg_o^{2+} inhibition between cortical receptors (composed of NR1, NR2A and NR2B) and NR1/2D receptors.

Methods

Cell culture

Human embryonic kidney (HEK) 293T cells (ATCC, Manassas, VA, USA) were used for whole-cell experiments and HEK293 cells (ATCC) were used for outside-out patch recordings. These choices were made because 293T cells provided larger whole-cell currents, whereas the success rate for pulling outside-out patches was much higher with HEK293 cells. The cells were cultured at 37°C in 5% CO_2–95% air. The culture medium for 293T cells was Dulbecco's modified Eagle's medium (DMEM) (Invitrogen Life Technologies, Carlsbad, CA, USA) with 5% fetal bovine serum (FBS) and 2 mM glutamine. The culture medium for HEK293 cells was DMEM with 10% FBS, 2 mM glutamine and 1 mM sodium pyruvate. The cells were maintained in 100-mm culture dishes and split twice a week. For experiments, the cells were plated onto glass coverslips pretreated with poly D-lysine (0.1 mg ml^{-1}) and rat-tail collagen (0.1 mg ml^{-1}, BD Biosciences, San Jose, CA, USA) in 35-mm culture dishes at 1–4 $\times$ 10^5 cells per dish.

Transfection

HEK293 or 293T cells were transiently transfected with cDNAs for rat NMDA receptor subunits 18–24 h after plating. cDNA for NMDA receptor subunits NR1–1a, NR2A and NR2D (Buller & Monaghan, 1997) were subcloned into mammalian expression vector pcDM8. cDNA of enhanced Green Fluorescent Protein (eGFP) (gift from Dr Mark Fleck, Albany Medical College, NY, USA) was cotransfected as a marker of successfully transfected cells. 293T cells were transfected using LipofectAMINE/PLUS reagents (Invitrogen). Briefly, transfection was performed by adding to each dish 1 ml serum-free medium containing 1 μg total DNA, 5 μl LipofectAMINE and 4 μl PLUS. The ratio of cDNA used was 1 eGFP : 3 NR1 : 6 NR2 (A or D). DL-2-amino-5-amino-5-phosphono-valeric acid (DL-APV, (200 μM) was added to prevent NMDA receptor mediated-excitotoxicity. The LipofectAMINE reagents have been reported to weaken the plasma membrane, presumably by incorporating into it, and consequently to be unsuitable for excised patch experiments (Groot-Kormelink *et al.* 2002). We therefore used a calcium phosphate precipitation procedure to transfect HEK293 cells. The amount of cDNA used per dish was 0.7 μg for eGFP, 0.7 μg for NR1–1a and

1.4 μg for NR2D. Precipitates were washed off with fresh culture medium that contained 200 μM DL-APV, 7–9 h after addition of DNA.

Solutions

Solutions were prepared daily from frozen stock and delivered using an in-house fabricated seven-barrel fast perfusion system (Qian *et al.* 2002). Currents were activated by 10 or 30 μM NMDA + 30 μM glycine. Mg^{2+} concentrations from 1 μM to 10 mM were added to external solutions. We did not adjust for changes in osmolality that resulted from adding Mg^{2+}. The external solution contained (mM): NaCl 140, $CaCl_2$ 1, KCl 2.8 and Hepes 10. The internal solutions contained (mM): CsCl 125, EGTA 10 and Hepes 10 for whole-cell experiments; CsF 115, CsCl 10, EGTA 10 and Hepes 10 for outside-out patch recordings. The pH of solutions was adjusted to between 7.1 and 7.2 using HCl or the basic form of the major charge carrier. Sucrose and *N*-methyl-D-glucamine were used to adjust the osmolality of external and internal solutions, respectively. The junction potentials between the pipette and bath solution were 5 mV in chloride-based internal solution and 9 mV for fluoride-based internal solution. All holding potentials were corrected for junction potentials. Ultrapure salts were used when available. All chemicals were from Sigma Chemical Co. (St Louis, MO, USA), except as indicated in the text.

Whole-cell recordings and analysis

Electrophysiological experiments were performed 20–72 h after transfection,. Whole-cell recordings were performed as previously described (Qian *et al.* 2002). Briefly, currents were recorded at room temperature with an Axopatch 200A or 200B amplifier (Axon Instruments, Foster City, CA, USA), low-pass filtered at 10 kHz, digitized at 44 kHz with a Neuro-Corder and stored on video tape for off-line analysis. Series resistance was compensated 60–80%. NMDA-activated currents in the absence ($I_{control}$) and presence (I_{Mg}) of multiple concentrations of Mg_o^{2+} were measured from −115 mV to −15 mV at 10 mV increments. The IC_{50} of Mg_o^{2+} at each voltage was estimated by fitting $I_{Mg}/I_{control}$ at various Mg_o^{2+} concentrations using eqn (1):

$$I_{Mg}/I_{control}(\%) = 100\%/\left[1 + \left([Mg^{2+}]_o/IC_{50}\right)^{n_H}\right] \quad (1)$$

IC_{50} and n_H (Hill coefficient) were not constrained (left as free parameters) during fitting. Curve fitting was performed using Origin 4.0 or 6.0 software (OriginLab Corp., Northampton, MA, USA). The IC_{50} value at each voltage was derived from fits to $I_{Mg}/I_{control}$ measurements with three to six different concentrations of Mg_o^{2+} and from three to 10 cells at each $[Mg^{2+}]_o$. Because in some cells it was not possible to measure I_{Mg} at each relevant $[Mg^{2+}]_o$, IC_{50} values were not estimated from each cell. Instead, at each voltage eqn (1) was fitted to pooled $I_{Mg}/I_{control}$ values, although for clarity only the mean values ± S.E.M. were plotted in Fig. 1*B*. Error bars in Fig. 1*C* show standard error estimated during non-linear curve fitting of eqn (1) by Origin.

Single-channel recording and analysis

Outside-out patch recordings were performed at room temperature according to standard methods (Hamill *et al.* 1981). Pipettes (resistance, 5–8 MΩ) were pulled from borosilicate standard-walled glass with filaments (Warner Instrument Corp., Portland, OR, USA). Pipettes were coated with Sylgard and fire-polished. Single-channel currents were recorded using an Axopatch200A or 200B patch-clamp amplifier, low-pass filtered at 10 kHz, digitized at 44 kHz with a Neuro-Corder and stored on video tape for later analysis. Data were collected at voltages from − 105 mV to −45 mV. At each voltage, single-channel currents in each patch were collected in 50–240 s segments, with the first segment being a control measurement in 0 Mg_o^{2+}, followed by one to three additional segments in different Mg_o^{2+} concetrations. Data from at least three patches were used at each voltage.

For analysis, each data segment recorded was played back, filtered at 2.5 kHz (−3 dB, eight-pole, low-pass bessel filter) and digitally sampled at 25 kHz using pCLAMP 8 Clampex software (Axon Instruments). The effective filter frequency was 2.43 kHz due to cascaded filters. NR1/2D receptor activation is characterized by relatively short open-duration (dominant mean open time, 0.67 ms) and frequent occupancy of subconductance states (see Fig. 2*A*). To permit accurate estimation of brief duration events and thereby minimize potential errors from missed events, we used the DC analysis programs (www.ucl.ac.uk/Pharmacology/dc/html), which make use of time-course fitting techniques (Colquhoun & Sigworth, 1995). Dwell-time histograms were plotted on square root *versus* log time scales (Sigworth & Sine, 1987). A chosen time resolution was applied to dwell-time distributions and durations shorter than the value of the time resolution were deleted from both open and closed-duration distributions. The resulting dwell-time histograms were fitted by the maximum likelihood method (Colquhoun & Sigworth, 1995) and the value of the imposed time resolution was subtracted from the time constants of the fit. The time resolution value was 50 μs in most patches (range, 45–85 μs), comparable to studies from other labs (for example Wyllie *et al.* 1996).

Open-duration histograms in the absence or presence of Mg_o^{2+} were fitted by one to three exponentials (Fig. 2*B* and *C*), consistent with previous studies (e.g. Wyllie *et al.* 1996; Wyllie *et al.* 1998). Of all open-duration histograms fitted, 20% were fitted by one, 48% by two, and 32% by

three components. The decrease of the time constant of the largest component (τ_o) with increasing $[Mg^{2+}]_o$ was used to estimate Mg_o^{2+} blocking rate (see Results). We did not further characterize the other exponential components. Because open periods (duration of openings regardless of current amplitude) were measured, each open event may contain transitions among openings of different amplitude levels. We did not analyse data from main and subconductance levels separately because of the difficulty of determining conductance level of brief events. To accurately determine the subconductance level of an opening the events must be of long enough duration (at least twice the filter rise time) to reach full amplitude. In NR1/2D receptors, many events were too short to meet this criterion.

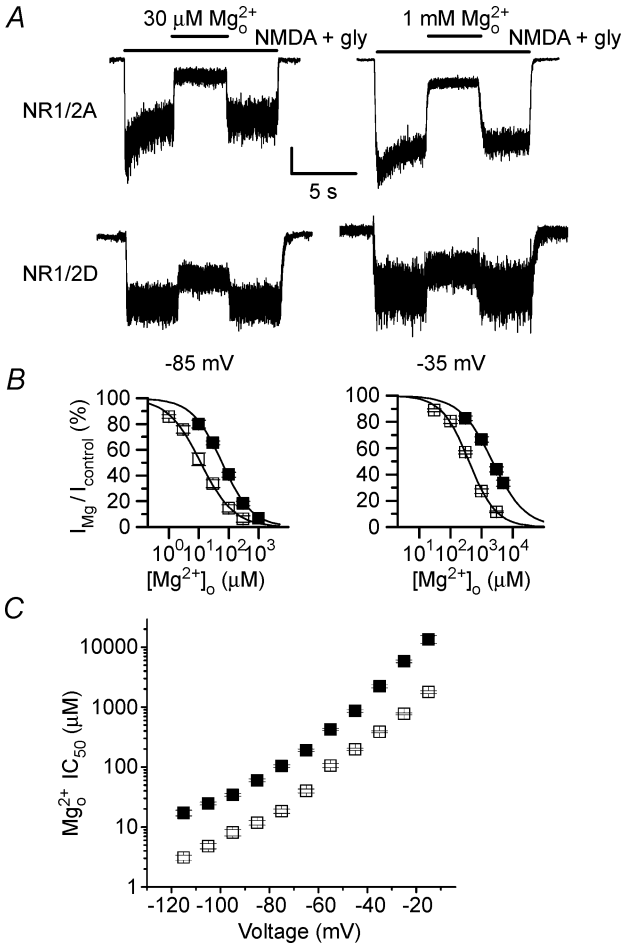

Figure 1. Mg_o^{2+} inhibition of NR1/2A- and NR1/2D-mediated whole-cell currents

A, Mg_o^{2+} inhibition of NMDA receptor-mediated whole-cell currents recorded from 293T cells transfected with NR1/2A (upper traces) and NR1/2D (lower traces) receptors. Bars above current traces show the times of application of the indicated solutions. At −85 mV (left traces), 30 μM Mg_o^{2+} inhibited NR1/2A receptor currents by 75% and NR1/2D receptor currents by 29%. At −35 mV (right traces), 1 mM Mg_o^{2+} inhibited NR1/2A receptors by 73% and NR1/2D receptors by 29%. Current scale bar is 100 pA except for bottom right trace, for which it is 20 pA. Traces are from four different cells. *B*, $[Mg^{2+}]_o$–inhibition curves plotted for NR1/2A (□) and NR1/2D (■) receptor currents at the indicated voltages. *C*, Mg_o^{2+} IC_{50} values measured from −115 to −15 mV plotted for NR1/2A (□) and NR1/2D (■) receptor currents.

Closed-duration histograms in the absence of Mg_o^{2+} were adequately fitted by the sum of three or four exponentials (Fig. 2*B* and *C*). In both the absence and presence of Mg_o^{2+}, closed-duration histograms included the duration of all closures, regardless of the conductance level from which the closure began. In the presence of Mg_o^{2+}, in most experiments an additional closed-duration component was observed (time constant, τ_b). This component was interpreted to represent blocking events by Mg_o^{2+} because its characteristics were typical of block: it was induced by the presence of Mg_o^{2+} and the value of τ_b was insensitive to $[Mg^{2+}]_o$ (Fig. 4). The mean amplitude of τ_b (30%) is significantly larger than the mean amplitude of the neighbouring, shorter, time constants (13.6%; $P = 0.004$) or the mean amplitude of the neighbouring, longer, time constants (12.4%; $P < 0.001$). Occasionally, when the value of τ_b was very close to the briefest closed-duration component observed in the absence of Mg_o^{2+}, the closed-duration histogram was fitted by the same number of exponentials in the absence and presence of Mg_o^{2+}. In those cases the value of τ_b still could be estimated with reasonable accuracy because the time constant of the confounding brief closed-duration component was necessarily close to τ_b, and because the amplitude of the τ_b component (mean of 33.7%) was relatively large (e.g. significantly larger than the neighbouring, longer time constant (17.3%; $P = 0.013$)).

The true mean duration of the main channel open state must be shorter than τ_o because missed brief closings cause neighbouring channel openings to be adjoined during data analysis. The same reasoning applies to overestimation of the mean duration of blocked state due to missed short openings. Because both open- and closed-duration histograms contained multiple components, correction for missed events was not practical (Colquhoun & Sigworth, 1995). To minimize errors introduced by missed events, we optimized our time resolution using time-course fitting (see above) and used only Mg_o^{2+} concentrations in which τ_o was substantially longer than the imposed time resolution values. The shortest τ_o measured was 0.228 ms, which was 4.6-fold longer than the time resolution in that patch. The shortest τ_b measured was 0.2 ms (3.3-fold longer than the time resolution). τ_b values were not dependent on $[Mg^{2+}]_o$ (Fig. 4*B*), suggesting that missed openings were not frequent enough to appreciably affect our estimates of τ_b. The observation that single channel-derived dissociation constant (K_D) values (see later) agreed well with IC_{50} values measured in whole-cell experiments over a 60 mV range (Fig. 6) also lends support to the accuracy of our measurements.

The apparent Mg_o^{2+} blocking and unblocking rates, $k_{+,app}$ and $k_{-,app}$ were estimated as described by Neher & Steinbach (1978). The term 'apparent' is used because Mg_o^{2+} blocking and unblocking rates as measured here are affected by permeant ions present in the internal and external solutions (Antonov & Johnson, 1999; Zhu & Auerbach, 2001*a*,b). $k_{+,app}$ was estimated from the eqn (2) by measuring the slope of a linear regression line fitted through a plot of $1/\tau_o$ *versus* $[Mg^{2+}]_o$ (Fig. 3*C*).

$$1/\tau_{o,Mg} = 1/\tau_{o,control} + k_{+,app}[Mg^{2+}]_o \qquad (2)$$

$k_{-,app}$ was estimated as $1/\tau_b$. Because $1/\tau_b$ should equal the sum of all rates for leaving the open-blocked state, this estimate assumes that closing rate(s) of blocked channel is low relative to $k_{-,app}$ (Antonov & Johnson, 1996). The accuracy of this assumption is difficult to evaluate because we have no way to estimate the closing rate(s) of blocked channels. If the assumption is incorrect, then $k_{-,app}$ would be slower, and K_D lower, than estimated here. Data are expressed as mean ± S.E.M.

Results

Mg_o^{2+} inhibition of NR1/2D receptor-mediated whole-cell currents

We first characterized Mg_o^{2+} inhibition of whole-cell NR1/2D responses and compared Mg_o^{2+} inhibition of NR1/2A and NR1/2D responses. Figure 1*A* shows current traces recorded at −85 mV (left) and −35 mV (right) from 293T cells transfected with NR1/2A (top) or NR1/2D (bottom) receptors. During a continuous application of agonist, a single concentration of Mg_o^{2+} was applied to inhibit currents. Mg_o^{2+} inhibited the currents rapidly in both receptor subtypes. At either voltage, NR1/2A receptor-mediated currents were inhibited much more effectively by $[Mg^{2+}]_o$ than NR1/2D receptor-mediated currents. Mg_o^{2+} concentration–inhibition curves were constructed to estimate the IC_{50} of Mg_o^{2+} at −85 and −35 mV (Fig. 1*B*). At either voltage, the concentration–inhibition curve for NR1/2D receptors was right-shifted relative to the curves

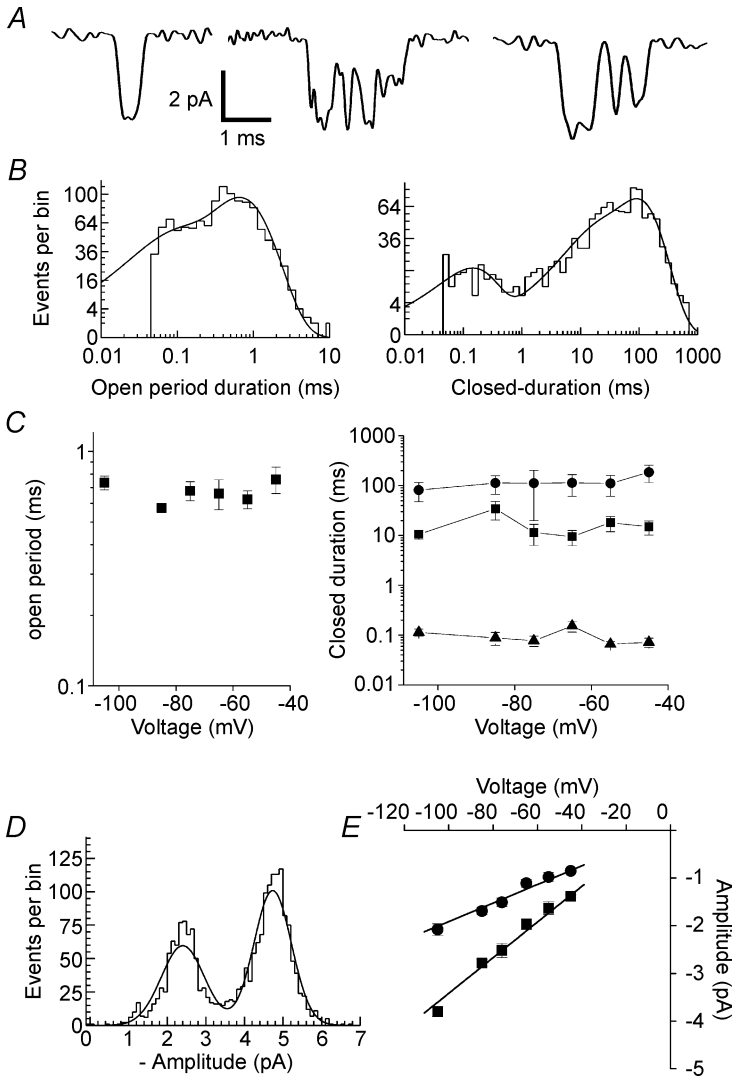

Figure 2. NR1/2D receptor single-channel properties in 0 Mg_o^{2+}
A, examples of NR1/2D receptor single-channel current traces recorded at −105 mV. *B*, open period (left) and closed-duration (right) histograms. Same patch as in *A*. The open period histogram was fitted by two exponentials with time constants of 60 μs (22.8%) and 655 μs (77.2%). The closed-duration histogram was fitted by four exponentials with time constants of 138 μs (15.2%), 11.7 ms (16%), 15.5 ms (2%) and 92.5 ms (66.8%). *C*, lack of voltage-dependence of the open period (left) and closed-duration (right) components that were observed in all patches. Time constants averaged across all voltages are: open period, 668 ± 30 μs; closed-duration, 94 ± 11 μs, 17.6 ± 3.6 ms and 124 ± 23 ms. *D*, example of amplitude histogram at −105 mV. Two Gaussian components were fitted to data with peaks at −2.44 pA (area, 40.4%) and at −4.73 pA. *E*, mean single-channel current plotted as a function of voltage. Unconstrained regression fits gave slope conductances of 19.5 and 37.4 pS and reversal potentials −1.6 and −5.5 mV, respectively.

for NR1/2A receptors. In Fig. 1*B*, the IC_{50} values for Mg_o^{2+} at −85 mV were 11.8 μM for NR1/2A and 60.0 μM for NR1/2D; at −35 mV, the values were 388 μM for NR1/2A and 2.22 mM for NR1/2D. These results are consistent with previous reports (Monyer *et al.* 1994; Kuner & Schoepfer, 1996; Momiyama *et al.* 1996) that Mg_o^{2+} inhibited NR1/2A receptor-mediated currents much more effectively than NR1/2D receptor-mediated currents.

Using the procedures shown in Fig. 1*B*, we measured the Mg_o^{2+} IC_{50} for both NR1/2A and NR1/2D receptor-mediated whole-cell currents from −115 mV to −15 mV at 10 mV intervals (Fig. 1*C* and Table 1). Mg_o^{2+} IC_{50} values are voltage-dependent in both receptor types, consistent with Mg_o^{2+} blocking both channel types by occupying a site within the voltage field. At each voltage tested, Mg_o^{2+} IC_{50} was at least 4-fold higher in NR1/2D than in NR1/2A receptors. Hill coefficient values showed no apparent voltage-dependence; when averaged over all voltages Hill coefficients for NR1/2A responses (0.87 ± 0.04) and for NR1/2D responses (0.86 ± 0.01) were nearly identical and suggested that block by Mg^{2+} is not cooperative.

The NR1/2A receptor Mg_o^{2+} IC_{50} values shown in Fig. 1*C* are very close to the Mg_o^{2+} IC_{50} values measured previously from native NMDA receptors in primary cultures of embryonic rat cortical neurones (referred to here as 'cortical receptors'; Qian *et al.* 2002). The mean value of the ratio (Mg_o^{2+} IC_{50}, cortical receptor response)/(Mg_o^{2+} IC_{50}, NR1/2A response), over the voltage range at which both were measured (−105 to −15 mV), is 1.4 ± 0.1 ($n = 10$). In contrast, from the data shown in Fig. 1*C*, the ratio (Mg_o^{2+} IC_{50}, NR1/2D response)/(Mg_o^{2+} IC_{50}, NR1/2A response) is 5.4 ± 0.4 ($n = 11$). These data strongly support previous biochemical and biophysical studies (e.g. Monyer *et al.* 1994; Zhong *et al.* 1994; Kirson & Yaari, 1996; Antonov & Johnson, 1999) demonstrating that the NR2 subunits expressed by embryonic cortical neurones (as used previously by Qian *et al.* 2002) are nearly exclusively NR2A or NR2B, which form receptors

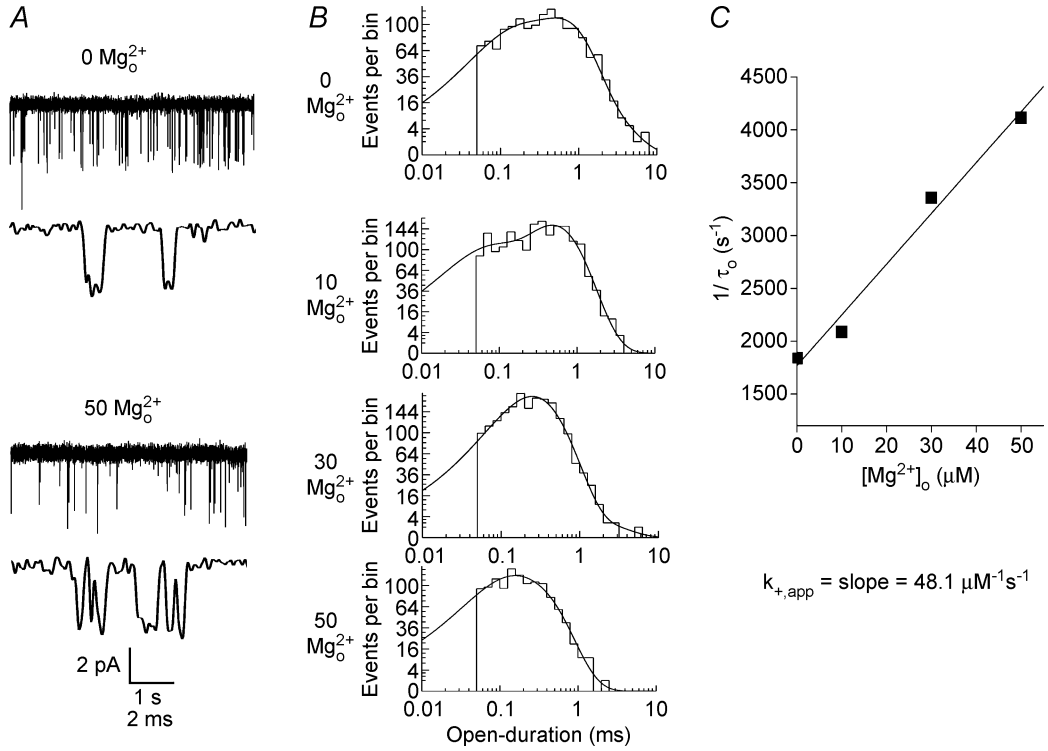

Figure 3. Effect of Mg_o^{2+} on open-duration histograms of NR1/2D receptors
A, single-channel recordings of NR1/2D receptor-mediated currents at −85 mV are shown in the presence of the indicated $[Mg^{2+}]_o$ at a slower (upper trace of each pair) and faster (lower traces) time base. *B*, open-duration histograms at −85 mV from the same patch as used for *A* in the presence of the indicated $[Mg^{2+}]_o$. Each histogram was fitted with three components except for in 50 μM Mg_o^{2+}, which was fitted with two components. In each $[Mg^{2+}]_o$, the time constant (and relative amplitude) of each component of the fits was: 0 Mg_o^{2+} 96 μs (28%), 0.54 ms (64%), 1.4 ms (9%); 10 μM Mg_o^{2+} 48 μs (28%), 0.48 ms (71%), 0.82 ms (1%); 30 μM Mg_o^{2+}, 147 μs (22%), 0.30 ms (76%), 1.1 ms (1%); 50 μM Mg_o^{2+}, 78 μs (31%), 0.24 ms (69%). *C*, the apparent blocking rate constant for Mg_o^{2+}, $k_{+,app}$, was estimated from the slope of a linear regression line fitted to a plot of $1/\tau_o$ *versus* $[Mg^{2+}]_o$.

that exhibit similar Mg_o^{2+} sensitivity (Monyer *et al.* 1994; Kuner & Schoepfer, 1996). The microscopic Mg_o^{2+} block kinetics of cortical receptors have been characterized in detail in this laboroatory (Antonov & Johnson, 1999). We next examined at the single-channel level the Mg_o^{2+} block kinetics of NR1/2D receptors, which later will be compared to our previous measurements of the kinetics of block of cortical receptors.

Mg_o^{2+} block of NR1/2D receptors at the single-channel level

Mg_o^{2+} IC_{50} measurements, although informative regarding the physiological extent of Mg_o^{2+} inhibition, do not reveal the underlying blocking kinetics, as IC_{50} values are related to the ratio of Mg_o^{2+} unblocking and blocking rates. We next characterized Mg_o^{2+} block at the single-channel level.

We first characterized the single-channel properties of NR1/2D receptors in the absence of Mg_o^{2+}. These control data are particularly important because, to our knowledge, measurements of the single-channel characteristics of NR1/2D receptors in a mammalian expression system have not been published. Single-channel traces at −105 mV (Fig. 2*A*) show that NR1/2D receptor channel openings are brief and open to both main and sub-conductance levels. The duration of the largest open duration component (Fig. 2*B*, left), the only component that was evident in all patches, was voltage-independent (Fig. 2*C*, left). The duration of the three closed duration components (Fig. 2*B*, right) that were evident in all patches also were voltage-independent (Fig. 2*C*, right). Thus, we detected no inherent voltage-dependence of gating of NR1/NR2D receptors. Amplitude histograms (Fig. 2*D*) were used to plot current–voltage (*i*–*V*) curves for the main and subconductance states (Fig. 2*E*), which exhibited voltage-independent conductances of 37.4 and 19.5 pS, respectively, and extrapolated reversal potentials near 0 mV. Except for the voltage-independence of dwell times of NR1/2D receptors, which has not previously been examined, the NR1/2D receptor characteristics shown in Fig. 2 are consistent with previous measurements in the oocyte expression system (Wyllie *et al.* 1996, 1998).

Addition of Mg_o^{2+} caused the brief NR1/2D receptor channel openings to appear 'flickery' (Fig. 3*A*), consistent with a channel blocker of intermediate kinetics (Hille, 2001). Channel flicker during Mg_o^{2+} block of NR1/2D receptors is less obvious than during Mg_o^{2+} block of NR1/2A or NR1/2B receptors because of the briefer open durations of NR1/2D receptors.

Mg_o^{2+}-induced changes in dwell-time distributions were used to examine the kinetics of Mg_o^{2+} block. Mg_o^{2+} blocking rates (see Methods) were estimated from open-duration histograms (Fig. 3*B*). In the control condition (0 Mg_o^{2+}) in Fig. 3*B*, the open-duration histogram was fitted by three exponential components. In the presence of each of the three concentrations of Mg_o^{2+} shown, open-duration histograms still were well fitted by three exponential components. The time constant of the main component, τ_o, declined as $[Mg^{2+}]_o$ increased. We did not further characterize the other two exponential components in different Mg_o^{2+} concentrations. As expected for a open channel blocker (Neher & Steinbach, 1978), the inverse of τ_o depends linearly on $[Mg^{2+}]_o$ (Fig. 3*C*). $k_{+,app}$ was estimated from the slope of the regression line through the data points.

Closed-duration histograms were used to estimate Mg_o^{2+} unblocking rate, $k_{-,app}$ (Fig. 4). In the example shown in Fig. 4*A*, the closed-duration distributions in control condition could be adequately fitted by four exponential components. In the presence of Mg_o^{2+}, an additional exponential component was needed to adequately fit the closed-duration histograms. The time constant of this additional component is τ_b (see Methods). $k_{-,app}$ was estimated by averaging the inverse of τ_b in 10, 30 and 50 μM Mg_o^{2+}. In contrast to $k_{+,app}$, $k_{-,app}$ is not correlated with $[Mg^{2+}]_o$ at any voltages ($P = 0.27$ at −85 mV; *P*-values range from 0.27 to 0.96).

Mechanistic differences between Mg_o^{2+} block of cortical and NR1/2D receptors

Measurements of Mg_o^{2+} $k_{+,app}$ and $k_{-,app}$ allowed us to probe the underlying mechanism of Mg_o^{2+} block of NR1/2D receptors. Both Mg_o^{2+} $k_{+,app}$ and $k_{-,app}$ are voltage-dependent. From −45 to −75 mV, $k_{-,app}$ (Fig. 5*A* and Table 1) decreased with hyperpolarization, consistent with a channel blocker that unblocks predominantly to the extracellular side of the membrane. From −75 to −105 mV, $k_{-,app}$ appeared to increase with hyperpolarization in NR1/2D receptors (not statistically significant; ANOVA, $P = 0.07$). This observation suggests that, at voltages more hyperpolarized than −75 mV, Mg_o^{2+} unblocks from NR1/2D receptors predominantly by permeating the channel Mg_o^{2+} $k_{+,app}$ decreased with depolarization (Fig. 5*B* and Table 1), as expected for an extracellular channel blocker.

To examine the differences in Mg_o^{2+} block between NR1/2D and cortical receptors, we compared results obtained from this study with previously published work on cortical receptors (Antonov & Johnson, 1999). The $k_{-,app}$ of NR1/2D receptors is much faster than the $k_{-,app}$ of cortical receptors at all voltages tested (Fig. 5*C*,●). The voltage-dependence of $k_{-,app}$ of NR1/2D was also distinct from cortical receptors: while the $k_{-,app}$ of NR1/2D goes through a minimum at −75 mV, the $k_{-,app}$ of cortical receptors only appears to become voltage-independent at voltages more negative than −80 mV (Antonov & Johnson, 1999). This difference between NR1/2D and

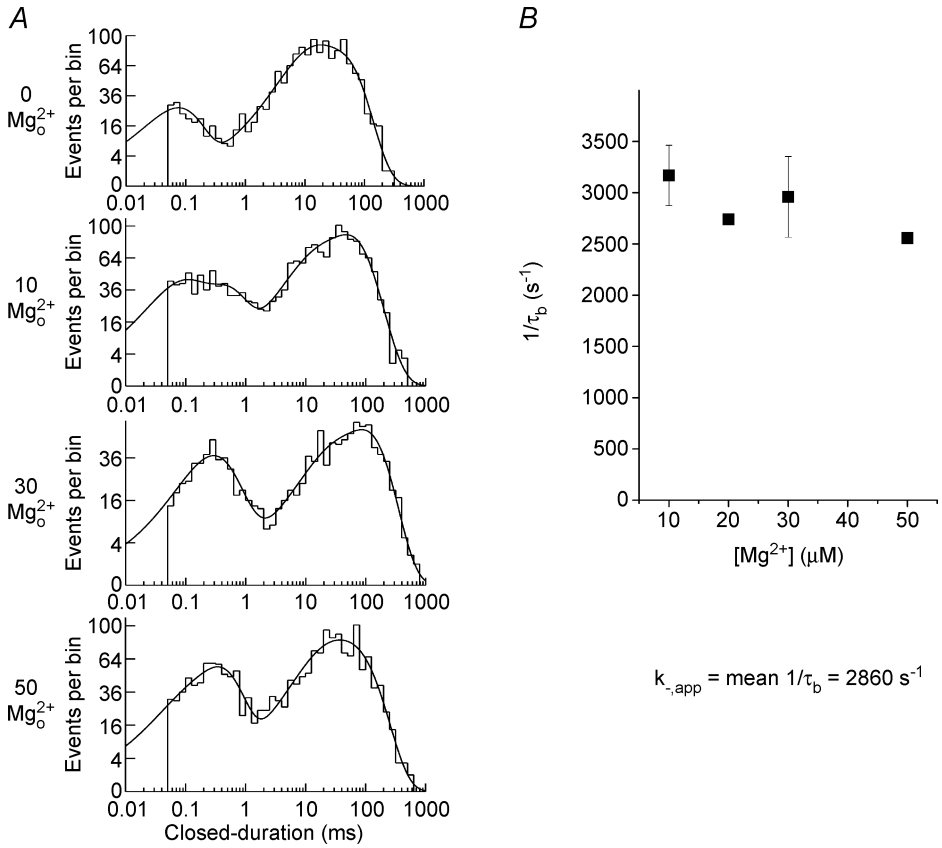

Figure 4. Effect of Mg_o^{2+} on closed-duration histograms of NR1/2D receptors
A, examples of closed-duration histograms at −85 mV in the presence of the indicated $[Mg^{2+}]_o$ from the patch used for Fig. 3. In the absence of Mg_o^{2+} the closed-duration histogram was fitted with four exponential components. In the presence of Mg_o^{2+} an additional component (time constant, τ_b) emerged in each of the histograms. The $[Mg^{2+}]_o$, value of τ_b and amplitude of τ_b are: 10 μM Mg_o^{2+} 0.372 ms, 19.4%; 30 μM Mg_o^{2+}, 0.255 ms, 23.5%; and 50 μM Mg_o^{2+}, 0.330 ms, 31.5%, respectively. *B*, the inverse of the mean duration of channel blocking events ($1/\tau_b$) is plotted as a function of $[Mg^{2+}]_o$ at −85 mV; $1/\tau_b$ did not depend on $[Mg^{2+}]_o$ at any voltage. Results are pooled from five experiments ($n = 3$, 1, 4, 2 at 10, 20, 30, 50 μM Mg_o^{2+}, respectively). The apparent unblocking rate for Mg_o^{2+}, $k_{-,app}$, was estimated as the mean value of $1/\tau_b$.

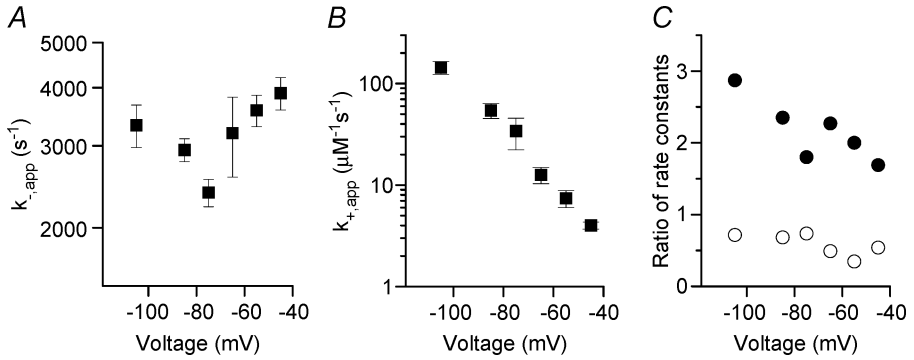

Figure 5. Voltage-dependence of rates of Mg_o^{2+} block and unblock
$k_{-,app}$ (*A*) and $k_{+,app}$ (*B*) for NR1/2D receptors are plotted as a function of voltage. *C*, the (NR1/2D receptor)/(cortical receptor) ratio for $k_{-,app}$ (●) and for $k_{+,app}$ (○) are plotted as a function of voltage. Data for cortical receptors were estimated by linear interpolation of data from Antonov & Johnson (1999). For example, $k_{-,app}$ at −105 mV for cortical receptors was estimated as the average of measurements at −100 and −110 mV by Antonov & Johnson (1999).

cortical receptors in the voltage-dependence of $k_{-,app}$ results in a steady decrease with depolarization in the $k_{-,app}$ ratio (Fig. 5*C*; slope of linear regression significantly different from 0; $P = 0.033$). The voltage-dependence of the $k_{+,app}$ of the two receptor types is similar, with $k_{+,app}$ of NR1/2D being moderately lower than the $k_{+,app}$ of cortical receptors at every voltage tested (Fig. 5*C*).

Therefore, Mg_o^{2+} inhibits NR1/2D receptors more weakly than cortical (NR1, NR2A and NR2B subunit-containing) NMDA receptors both because block is slower and unblock is faster for NR1/2D receptors. The predominant difference that underlies the NR2 subunit-dependence of inhibition is faster Mg_o^{2+} unblock from NR1/2D receptors.

Effect of Mg_o^{2+} block on equilibria between kinetic states of NR1/2D receptors

We examined the relationship between Mg_o^{2+} IC_{50} values measured from whole-cell experiments (see Fig. 1) and microscopic Mg_o^{2+} K_D values calculated from single-channel experiments using the relationship $K_D = k_{-,app}/k_{+,app}$. At each voltage at which IC_{50}, $k_{-,app}$ and $k_{+,app}$ were measured, Mg_o^{2+} IC_{50} and K_D values are comparable (Fig. 6). The similarity between the two data sets at all voltages supports the accuracy of our single-channel measurements. In addition, the equality of IC_{50} and K_D suggests that, as was previously reported for cortical receptors (Qian *et al.* 2002), Mg_o^{2+} block does not affect the equilibria between kinetic states of NR1/2D receptors.

Discussion

The biophysical properties of NR1/2D (as well as NR1/2C) receptors has been far less extensively investigated than those of NR1/2A and NR1/2B receptors. However several intriguing aspects of NR1/2D receptor gating have been reported: the extremely slow deactivation of NMDA receptors after glutamate removal (Monyer *et al.* 1992; Vicini *et al.* 1998; Wyllie *et al.* 1998); the prominent subconductance state (Wyllie *et al.* 1996; Misra *et al.* 2000); and the asymmetry in transitions between the main- and sub-conductance states (Wyllie *et al.* 1996; Misra *et al.* 2000). In the work reported here, we focused on Mg_o^{2+} block of NR1/2D receptors, a fundamental property of NMDA receptors. The main results are: (1) voltage-dependent inhibition by Mg_o^{2+} of whole-cell currents was weaker for NR1/2D than NR1/2A receptors at all voltages tested. (2) Mg_o^{2+} $k_{+,app}$ was moderately slower in NR1/2D than cortical receptors, but the voltage-dependence was similar in the two receptor types. (3) Mg_o^{2+} $k_{-,app}$ was much faster for NR1/2D than cortical receptors at all voltages tested. (4) The voltage-dependence of the Mg_o^{2+} $k_{-,app}$ of NR1/2D and cortical receptors differed. In contrast to data from cortical receptors, the Mg_o^{2+} $k_{-,app}$ of NR1/2D receptors appeared to go through a minimum at −75 mV. The difference between the Mg_o^{2+} $k_{-,app}$ of NR1/2D and cortical receptors decreased with depolarization. (5) The Mg_o^{2+} IC_{50} of NR1/2D receptors measured with whole-cell experiments was in excellent agreement with the K_D value obtained from single-channel experiments at all voltages tested.

Comparison with previous studies

The molecular mechanism of the NR2 subunit-dependence of inhibition of whole-cell NMDA currents by Mg_o^{2+} has been studied in *Xenopus laevis* oocytes (Kuner & Schoepfer, 1996). In general, the data presented here and the findings of Kuner & Schoepfer (1996) are similar: both studies reported voltage-dependent inhibition by Mg_o^{2+} that is stronger in NR1/2A than NR1/2D receptors. However, there are some notable differences between the studies. In our study, Mg_o^{2+} inhibition was substantially weaker in NR1/2D than in NR1/2A receptors at all voltages tested (Fig. 1*C*) while in the experiments of Kuner & Schoepfer (1996), Mg_o^{2+} IC_{50} values tended to converge at depolarized voltages. The absolute values of Mg_o^{2+} IC_{50} were also lower in their studies. For example, IC_{50} of NR1/2D receptors at −70 mV is estimated to be about 55 μM by Kuner & Schoepfer (1996) and 145 μM in this study.

We do not know the reasons for these differences. The accuracy of our whole-cell measurements is supported by the very similar IC_{50} values and voltage-dependence of Mg_o^{2+} inhibition measured in two different mammalian systems, 293T cells and rat cortical neurones. One possibility is that differences in results of this study and that of Kuner & Schoepfer (1996) are due to differences in

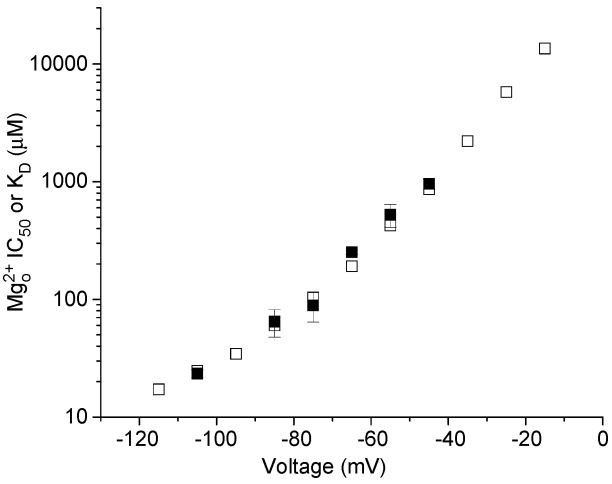

Figure 6. Voltage-dependence of Mg_o^{2+} IC_{50} and K_D in NR1/2D receptors
Mg_o^{2+} IC_{50} (□) measured from whole-cell experiments and K_D (■) calculated from single-channel experiments ($K_D = k_{-,app}/k_{+,app}$) are plotted for NR1/2D receptors. The values of Mg_o^{2+} IC_{50} and K_D are comparable over the voltage range measured.

Table 1. Voltage-dependence of measured values of IC_{50}, $k_{+,app}$, and $k_{-,app}$

Voltage (mV)	NR1/2A IC_{50} (μM)	NR1/2D IC_{50} (μM)	NR1/2D $k_{+,app}$ (μM^{-1} s^{-1})	NR1/2D $k_{-,app}$ (s^{-1})
−15	1780	13500	—	—
−25	773	5790	—	—
−35	388	2220	—	—
−45	198	863	4	3893
−55	106	425	7.4	3575
−65	40	191	12.6	3194
−75	18.4	104	34	2380
−85	11.8	60	54.3	2940
−95	8.1	34.4	—	—
−105	4.8	24.7	144	3323
−115	3.1	17.2	—	—

Parameter values not measured are indicated with a dash.

permeant ion concentrations. Previous studies (Antonov & Johnson, 1999; Zhu & Auerbach, 2001*a*,*b*; Qian *et al.* 2002) have shown that permeant ion concentrations shape both the affinity and voltage-dependence of Mg_o^{2+} block. The internal ion concentration in oocytes are likely to be significantly different from the ion concentrations used in whole-cell recordings. In addition, the kind of permeant intracellular ions present may influence Mg_o^{2+} block. Zhu & Auerbach (2001*b*) showed that internal K^+ can accelerate Mg_o^{2+} unblocking rate, while this effect was not observed with Cs^+ as the main internal cation (Antonov & Johnson, 1999). It is also possible that the difference in experimental preparation is a source of variability in results. We surveyed published Mg_o^{2+} IC_{50} values for NR1/2A and NR1/2D receptors, and found surprising variation in values measured in the oocyte expression system. In the relevant publications we found, IC_{50} values varied from as much as 15-fold lower than those reported here (Burnashev *et al.* 1992; Kawajiri & Dingledine, 1993; Sakurada *et al.* 1993; Kuner & Schoepfer, 1996; Kupper *et al.* 1996; Wagner & Leonard, 1996; Williams *et al.* 1998; Liu *et al.* 2001*b*) to as much as 15-fold higher (Wagner & Leonard, 1996; Liu *et al.* 2001*a*; Wyllie *et al.* 1996). Previous measurements in HEK293 cells are far more limited; two publications gave values within a factor of 1.6 of those reported here (Wollmuth *et al.* 1998; Buck *et al.* 2000). Note that we could find no whole-cell HEK293 measurements of the Mg_o^{2+} IC_{50} of NR1/2D. Thus, there may be an unrecognized source of variability in measurements in the oocyte expression system of Mg_o^{2+} IC_{50} that complicates comparison of our results with those of previous publications. In contrast, previous measurements of other biophysical properties of NR1/2D receptors in oocytes, such as single-channel conductance and dwell-times (Wyllie *et al.* 1996, 1998), are consistent with those reported here (Fig. 2). A similar conclusion has been drawn for NR1/2A receptors (Stern *et al.* 1994).

Properties of Mg_o^{2+} block in NR1/2D receptors

We examined the properties of Mg_o^{2+} block in NR1/2D receptors using the dual approaches of whole-cell and single-channel recordings. Whole-cell recording of NR1/2D receptor currents revealed the voltage dependence of IC_{50}, but provided no kinetic information (Fig. 1). Single-channel recordings (Fig. 3*A*) suggested that Mg_o^{2+} caused flickers in channel openings, a characteristic typical of blockers of intermediate kinetics (Hille, 2001). Measurements of $k_{-,app}$ and $k_{+,app}$ (Figs 3 and 4) confirmed that Mg_o^{2+} block in NR1/2D receptors, as in cortical receptors, is of intermediate kinetics.

Channel blockers typically interact with channel gating transitions. Blockers that have the extreme effect of preventing channel closure are often called 'sequential blockers'. Channel blockers termed 'trapping blockers' allow the channel to close and trap the blocker. Many trapping blockers also affect channel gating (see Johnson & Qian, 2002). A method for estimating the effect of a blocker on the equilibrium between receptor states is to compare IC_{50} values from whole-cell experiments and K_D values from single-channel experiments. If the equilibrium between each pair of states is the same whether or not blocker is bound, then $IC_{50} = K_D$ (Johnson & Qian, 2002). Sequential blockers, on the other hand, prolong channel openings by holding the channel in the open state while blocker is bound, increasing the IC_{50} value of the sequential blocker (Johnson & Qian, 2002). IC_{50} to K_D ratios as high as 60 have been measured for blockers that inhibit channel closure (Sobolevsky, 2003). We show here that there is excellent agreement between the values of IC_{50} and K_D for NR1/2D receptors at all voltages tested (Fig. 6), as is the case for cortical receptors (Qian *et al.* 2002). This observation suggests that channel occupation by Mg_o^{2+} does not affect the equilibrium between states of NMDA receptors, which would be simply achieved if block by Mg_o^{2+} does not

affect receptor kinetics. However, equality of IC_{50} and K_D values would also be observed if Mg_o^{2+} block has compensatory effects on multiple equilibrium or kinetic constants, for example by slowing channel opening and closing equally. The idea that Mg_o^{2+} block does not affect NMDA receptor gating kinetics is also supported by Sobolevsky & Yelshansky (2000). However, recent studies of NMDA receptors in cortical neurones have suggested that Mg_o^{2+} block does affect the kinetics of NMDA receptor state transitions (Vargas-Caballero & Robinson, 2003, 2004; Kampa *et al.* 2004). Resolution of these conflicting conclusions will require further research.

Differences between Mg_o^{2+} inhibition of cortical and NR1/2D receptors

Mg_o^{2+} inhibition is weaker in NR1/2D than in NR1/2A or NR1/2B receptors. The mechanistic basis of this subunit-dependent difference was addressed by measuring Mg_o^{2+} blocking and unblocking rate constants in single-channel experiments. Our results show that the rates of Mg_o^{2+} block of NR1/2D receptors are moderately slower than the rates of block of cortical receptors over a wide range of voltages (Fig. 5*C*). Mg_o^{2+} unblocks much more rapidly from NR1/2D receptors than from cortical receptors. Consequently, the weaker Mg_o^{2+} inhibition of NR1/2D receptors is primarily the result of faster unblocking rates.

The Mg_o^{2+} $k_{-,app}$ of NR1/2D receptors decreases with hyperpolarization from −45 to −75 mV, suggesting that in this voltage range Mg_o^{2+} unblocks predominantly to the external solution. However, $k_{-,app}$ then goes through a minimum value and increases with further hyperpolarization (Fig. 5*A*). This observation indicates that Mg_o^{2+} unblocks predominantly to the internal solution (permeates) at voltages more hyperpolarized than −75 mV. Previous studies have suggested that Mg_o^{2+} can permeate native NMDA receptors (Mayer & Westbrook, 1987; Stout *et al.* 1996). A model of Mg_o^{2+} block based on single-channel measurements indicated that, when permeant ions are at physiological concentrations, the predominant direction of Mg_o^{2+} unblock from cortical receptors changes from outward to inward at about −105 mV (Antonov & Johnson, 1999). Using this model, the ratio of $k_{-,app}$ of NR1/2D and cortical receptors (Fig. 5*C*) can be reproduced by simply setting the NR1/2D receptor Mg_o^{2+} permeation rate to be about five times faster than the corresponding rate for cortical receptors (not shown). No change in the voltage-dependence of any rate constant is needed. This explanation surely is an oversimplification, given the multiple external and internal regions of NMDA receptors that have been reported to influence the NR2 subunit-dependence of inhibition by Mg_o^{2+} (Kuner & Schoepfer, 1996). However, our data are consistent with the idea that Mg_o^{2+} inhibits NR1/2D receptors less effectively than cortical receptors in part because of faster Mg^{2+} permeation of NR1/2D receptors. This conclusion would suggest that one of the regions identified by Kuner & Schoepfer (1996) to be responsible for NR2 subunit-dependence of inhibition by Mg_o^{2+} contributes to the energy barrier between the Mg_o^{2+} binding site and the internal solution.

References

Antonov SM & Johnson JW (1996). Voltage–dependent interaction of open-channel blocking molecules with gating of NMDA receptors in rat cortical neurons. *J Physiol* **493**, 425–445.

Antonov SM & Johnson JW (1999). Permeant ion regulation of N-methyl-D-aspartate receptor channel block by Mg^{2+}. Proc Natl Acad Sci U S A **96**, 14571–14576.

Ascher P & Nowak L (1988). The role of divalent cations in the N-methyl-D-aspartate responses of mouse central neurones in culture. *J Physiol* **399**, 247–266.

Bear MF, Kleinschmidt A, Gu QA & Singer W (1990). Disruption of experience-dependent synaptic modifications in striate cortex by infusion of an NMDA receptor antagonist. *J Neurosci* **10**, 909–925.

Bengzon J, Okabe S, Lindvall O & McKay RD (1999). Suppression of epileptogenesis by modification of N-methyl-D-aspartate receptor subunit composition. *Eur J Neurosci* **11**, 916–922.

Bliss TV & Collingridge GL (1993). A synaptic model of memory: long-term potentiation in the hippocampus. *Nature* **361**, 31–39.

Brickley SG, Misra C, Mok MH, Mishina M & Cull-Candy SG (2003). NR2B and NR2D subunits coassemble in cerebellar Golgi cells to form a distinct NMDA receptor subtype restricted to extrasynaptic sites. *J Neurosci* **23**, 4958–4966.

Buck DP, Howitt SM & Clements JD (2000). NMDA channel gating is influenced by a tryptophan residue in the M2 domain but calcium permeation is not altered. *Biophys J* **79**, 2454–2462.

Buller AL & Monaghan DT (1997). Pharmacological heterogeneity of NMDA receptors: characterization of NR1a/NR2D heteromers expressed in *Xenopus* oocytes. *Eur J Pharmacol* **320**, 87–94.

Burnashev N, Schoepfer R, Monyer H, Ruppersberg JP, Gunther W, Seeburg PH & Sakmann B (1992). Control by asparagine residues of calcium permeability and magnesium blockade in the NMDA receptor. *Science* **257**, 1415–1419.

Chapman AG (2000). Glutamate and epilepsy. *J Nutr* **130**, 1043S–1045S.

Cline HT, Debski EA & Constantine-Paton M (1990). The role of the NMDA receptor in the development of the frog visual system. *Adv Exp Med Biol* **268**, 197–203.

Colquhoun D & Sigworth FJ (1995). Fitting and statistical analysis of single-channel records. In *Single-Channel Recording*, ed. Sakmann B & Neher E, pp. 483–587. Plenum Press, New York.

Cull-Candy S, Brickley S & Farrant M (2001). NMDA receptor subunits: diversity, development and disease. *Curr Opin Neurobiol* **11**, 327–335.

Dingledine R, Borges K, Bowie D & Traynelis SF (1999). The glutamate receptor ion channels. *Pharmacol Rev* **51**, 7–61.

Erisir A & Harris JL (2003). Decline of the critical period of visual plasticity is concurrent with the reduction of NR2B subunit of the synaptic NMDA receptor in layer 4. *J Neurosci* **23**, 5208–5218.

Gardoni F, Pagliardini S, Setola V, Bassanini S, Cattabeni F, Battaglia G & Di Luca M (2003). The NMDA receptor complex is altered in an animal model of human cerebral heterotopia. *J Neuropathol Exp Neurol* **62**, 662–675.

Groot-Kormelink PJ, Beato M, Finotti C, Harvey RJ & Sivilotti LG (2002). Achieving optimal expression for single channel recording: a plasmid ratio approach to the expression of alpha 1 glycine receptors in HEK293 cells. *J Neurosci Methods* **113**, 207–214.

Hamill OP, Marty A, Neher E, Sakmann B & Sigworth FJ (1981). Improved patch-clamp techniques for high-resolution current recording from cells and cell-free membrane patches. *Pflugers Arch* **391**, 85–100.

Hille B (2001). *Ion Channels of Excitable Membranes*. Sinauer Associates, Inc, Sunderland, MA, USA.

Hrabetova S, Serrano P, Blace N, Tse HW, Skifter DA, Jane DE, Monaghan DT & Sacktor TC (2000). Distinct NMDA receptor subpopulations contribute to long-term potentiation and long-term depression induction. *J Neurosci* **20**, RC81.

Iwasato T, Datwani A, Wolf AM, Nishiyama H, Taguchi Y, Tonegawa S, Knopfel T, Erzurumlu RS & Itohara S (2000). Cortex-restricted disruption of NMDAR1 impairs neuronal patterns in the barrel cortex. *Nature* **406**, 726–731.

Johnson JW & Qian A (2002). Interaction between channel blockers and channel gating of NMDA receptors. *Biol ogicheskie Membrany* **19**, 17–22.

Kampa BM, Clements J, Jonas P & Stuart GJ (2004). Kinetics of Mg^{2+} unblock of NMDA receptors: implications for spike-timing dependent synaptic plasticity. *J Physiol* **556**, 337–345.

Kawajiri S & Dingledine R (1993). Multiple structural determinants of voltage-dependent magnesium block in recombinant NMDA receptors. *Neuropharmacology* **32**, 1203–1211.

Kirson ED & Yaari Y (1996). Synaptic NMDA receptors in developing mouse hippocampal neurones: functional properties and sensitivity to ifenprodil. *J Physiol* **497**, 437–455.

Kuner T & Schoepfer R (1996). Multiple structural elements determine subunit specificity of Mg^{2+} block in NMDA receptor channels. *J Neurosci* **16**, 3549–3558.

Kupper J, Ascher P & Neyton J (1996). Probing the pore region of recombinant N-methyl-D-aspartate channels using external and internal magnesium block. *Proc Natl Acad Sci U S A* **93**, 8648–8653.

Lisman JE & McIntyre CC (2001). Synaptic plasticity: a molecular memory switch. *Curr Biol* **11**, R788–R791.

Liu HT, Hollmann MW, Liu WH, Hoenemann CW & Durleux ME (2001*a*). Modulation of NMDA receptor function by ketamine and magnesium: Part I. *Anesthesia & Analgesia* **92**, 1173–1181.

Liu Y, Hill RH, Arhem P & von Euler G (2001*b*). NMDA and glycine regulate the affinity of the Mg^{2+}-block site in NR1-1a/NR2A NMDA receptor channels expressed in Xenopus oocytes. *Life Sciences* **68**, 1817–1826.

Mayer ML & Westbrook GL (1987). Permeation and block of N-methyl-D-aspartic acid receptor channels by divalent cations in mouse cultured central neurones. *J Physiol* **394**, 501–527.

Mayer ML, Westbrook GL & Guthrie PB (1984). Voltage-dependent block by Mg^{2+} of NMDA responses in spinal cord neurones. *Nature* **309**, 261–263.

Meldrum BS (1992). Excitatory amino acid receptors and disease. *Curr Opin Neurol Neurosurg* **5**, 508–513.

Misra C, Brickley SG, Wyllie DJ & Cull-Candy SG (2000). Slow deactivation kinetics of NMDA receptors containing NR1 and NR2D subunits in rat cerebellar Purkinje cells. *J Physiol* **525**, 299–305.

Miyamoto Y, Yamada K, Noda Y, Mori H, Mishina M & Nabeshima T (2002). Lower sensitivity to stress and altered monoaminergic neuronal function in mice lacking the NMDA receptor epsilon 4 subunit. *J Neurosci* **22**, 2335–2342.

Momiyama A, Feldmeyer D & Cull-Candy SG (1996). Identification of a native low-conductance NMDA channel with reduced sensitivity to Mg^{2+} in rat central neurones. *J Physiol* **494**, 479–492.

Monyer H, Burnashev N, Laurie DJ, Sakmann B & Seeburg PH (1994). Developmental and regional expression in the rat brain and functional properties of four NMDA receptors. *Neuron* **12**, 529–540.

Monyer H, Sprengel R, Schoepfer R, Herb A, Higuchi M, Lomeli H, Burnashev N, Sakmann B & Seeburg PH (1992). Heteromeric NMDA receptors: molecular and functional distinction of subtypes. *Science* **256**, 1217–1221.

Mori H, Masaki H, Yamakura T & Mishina M (1992). Identification by mutagenesis of a Mg^{2+}-block site of the NMDA receptor channel. *Nature* **358**, 673–675.

Nakazawa K, Quirk MC, Chitwood RA, Watanabe M, Yeckel MF, Sun LD, Kato A, Carr CA, Johnston D, Wilson MA & Tonegawa S (2002). Requirement for hippocampal CA3 NMDA receptors in associative memory recall. *Science* **297**, 211–218.

Neher E & Steinbach JH (1978). Local anaesthetics transiently block currents through single acetylcholine-receptor channels. *J Physiol* **277**, 153–176.

Nowak L, Bregestovski P, Ascher P, Herbet A & Prochiantz A (1984). Magnesium gates glutamate-activated channels in mouse central neurones. *Nature* **307**, 462–465.

Okabe S, Collin C, Auerbach JM, Meiri N, Bengzon J, Kennedy MB, Segal M & McKay RD (1998). Hippocampal synaptic plasticity in mice overexpressing an embryonic subunit of the NMDA receptor. *J Neurosci* **18**, 4177–4188.

Qian A, Antonov SM & Johnson JW (2002). Modulation by permeant ions of Mg^{2+} inhibition of NMDA-activated whole-cell currents in rat cortical neurons. *J Physiol* **538**, 65–77.

Ramoa AS, Mower AF, Liao D & Jafri SI (2001). Suppression of cortical NMDA receptor function prevents development of orientation selectivity in the primary visual cortex. *J Neurosci* **21**, 4299–4309.

Sakurada K, Masu M & Nakanishi S (1993). Alteration of Ca^{2+} permeability and sensitivity to Mg^{2+} and channel blockers by a single amino acid substitution in the *N*-methyl-D-aspartate receptor. *J Biol Chem* **268**, 410–415.

Sigworth FJ & Sine SM (1987). Data transformations for improved display and fitting of single-channel dwell time histograms. *Biophys J* **52**, 1047–1054.

Sobolevsky AI (2003). Channel block of glutamate receptors. In *Recent Research Developments in Physiology Vol. 1 Part I,* ed. Pandalai SG, pp. 1–38, Research Signpost, Kerala, India.

Sobolevsky AI & Yelshansky MV (2000). The trapping block of NMDA receptor channels in acutely isolated rat hippocampal neurones. *J Physiol* **526**, 493–506.

Stern P, Behe P, Schoepfer R & Colquhoun D (1992). Single-channel conductances of NMDA receptors expressed from cloned cDNAs: comparison with native receptors. *Proc R Soc Lond B Biol Sci* **250**, 271–277.

Stern P, Cik M, Colquhoun D & Stephenson FA (1994). Single channel properties of cloned NMDA receptors in a human cell line: comparison with results from Xenopus oocytes. *J Physiol* **476**, 391–397.

Stout AK, Li-Smerin Y, Johnson, JW & Reynolds IJ (1996). Mechanisms of glutamate-stimulated Mg^{2+} influx and subsequent Mg^{2+} efflux in rat forebrain neurones in culture. *J Physiol* **492**, 641–657.

Tang YP, Shimizu E, Dube GR, Rampon C, Kerchner GA, Zhuo M, Liu G & Tsien JZ (1999). Genetic enhancement of learning and memory in mice. *Nature* **401**, 63–69.

Tsai G & Coyle JT (2002). Glutamatergic mechanisms in schizophrenia. *Annu Rev Pharmacol Toxicol* **42**, 165–179.

Vargas-Caballero M & Robinson HPC (2003). A slow fraction of Mg^{2+} unblock of NMDA receptors limits their contribution to spike generation in cortical pyramidal neurons. *J Neurophysiol* **89**, 2778–2783.

Vargas-Caballero M & Robinson HPC (2004). Fast and slow voltage-dependent dynamics of magnesium block in the NMDA receptor: the asymmetric trapping block model. *J Neurosci* **24**, 6171–6180.

Vicini S, Wang JF, Li JH, Zhu WJ, Wang YH, Luo JH, Wolfe BB & Grayson DR (1998). Functional and pharmacological differences between recombinant N-methyl-D-aspartate receptors. *J Neurophysiol* **79**, 555–566.

Wagner DA & Leonard JP (1996). Effect of protein kinase-C activation on the Mg^{2+}-sensitivity of cloned NMDA receptors. *Neuropharmacology* **35**, 29–36.

Williams K, Pahk AJ, Kashiwagi K, Masuko T, Nguyen ND & Igarashi K (1998). The selectivity filter of the *N*-methyl-D-aspartate receptor: a tryptophan residue controls block and permeation of Mg^{2+}. *Mol Pharmacol* **53**, 933–941.

Wollmuth LP, Kuner T & Sakmann B (1998). Adjacent asparagines in the NR2-subunit of the NMDA receptor channel control the voltage-dependent block by extracellular Mg^{2+}. *J Physiol* **506**, 13–32.

Wyllie DJ, Behe P & Colquhoun D (1998). Single-channel activations and concentration jumps: comparison of recombinant NR1a/NR2A and NR1a/NR2D NMDA receptors. *J Physiol* **510**, 1–18.

Wyllie DJ, Behe P, Nassar M, Schoepfer R & Colquhoun D (1996). Single-channel currents from recombinant NMDA NR1a/NR2D receptors expressed in Xenopus oocytes. *Proc R Soc Lond B Biol Sci* **263**, 1079–1086.

Zeron MM, Hansson O, Chen N, Wellington CL, Leavitt BR, Brundin P, Hayden MR & Raymond LA (2002). Increased sensitivity to N-methyl-D-aspartate receptor-mediated excitotoxicity in a mouse model of Huntington's disease. *Neuron* **33**, 849–860.

Zhong J, Russell SL, Pritchett DB, Molinoff PB & Williams K (1994). Expression of mRNAs encoding subunits of the N-methyl-D-aspartate receptor in cultured cortical neurons. *Mol Pharmacol* **45**, 846–853.

Zhu Y & Auerbach A (2001*a*). Na^{+} occupancy and Mg^{2+} block of the *N*-methyl-D-aspartate receptor channel. *J Gen Physiol* **117**, 275–286.

Zhu Y & Auerbach A (2001*b*). K^{+} occupancy of the *N*-methyl-D-aspartate receptor channel probed by Mg^{2+} block. *J Gen Physiol* **117**, 287–298.

Acknowledgements

The authors thank Maria Pugh for her technical support and Dr David Colquhoun for providing analysis software and advice. This work was supported by National Institute of Mental Health grants MH45817 and MH00944 to J.W.J and predoctoral National Research Service Award MH12476 to A.Q.